

Thermodynamic analysis of temperature-graded ferroelectrics

S. P. Alpay^{a)} and Z.-G. Ban

*Department of Metallurgy and Materials Engineering and Institute of Materials Science,
University of Connecticut, Storrs, Connecticut 06269*

J. V. Mantese

Delphi Research Laboratories, Shelby Township, Michigan 48315

(Received 4 November 2002; accepted 4 January 2003)

A Landau–Ginzburg thermodynamic model is constructed and used to develop a methodology for analyzing temperature-graded ferroelectrics. Spatial nonuniformities in temperature are shown to give rise to nonuniformities in polarization with corresponding spatial variations. The magnitude and the sign of the polarization gradients are shown to depend on the imposed temperature gradient. The polarization gradients result in asymmetric hysteresis responses with “up” or “down” charge offsets. The theoretical analysis presented here not only predicts the general trends associated with the hysteresis offsets observed from temperature-graded ferroelectrics, but is also in excellent quantitative agreement with the experimental data reported in the literature [W. Fellberg, J. V. Mantese, N. W. Schubring, and A. L. Micheli, *Appl. Phys. Lett.* **78**, 524 (2001)]. © 2003 American Institute of Physics. [DOI: 10.1063/1.1556565]

In recent years, there has been great interest in graded ferroelectrics as they exhibit behavior and properties that are not observed in homogenous bulk or thin film ferroelectrics. Polarization-graded ferroelectrics are distinguished from homogenous ferroelectrics by a spatial variation of the electric dipole moment.¹ In addition, unlike homogeneous ferroelectrics, which are characterized by symmetric hysteresis loops with respect to the polarization and applied field axes, graded ferroelectric devices display strikingly different behavior; the most notable being a translation of the hysteresis loop along the polarization axis.^{2–4} The shifted charge–voltage hysteresis (“up” and “down”) loops are attributed to “built-in” potentials, analogous to the asymmetric current–voltage characteristics resulting from the “built-in” potential across chemically doped regions in semiconductor diode junctions. The graded structures, therefore, have given rise to a particular class of transcapacitive ferroelectric devices (or “transcapacitors”), having potential applications in infrared detection, actuation, and energy storage.

Heretofore, the great majority of polarization-graded ferroelectrics have been formed by chemically varying the composition of a base ferroelectric along a line normal to the electrodes when configured as capacitive structures. Recently, however, experimental work has been carried out to examine the hysteresis offset observed from temperature-graded bulk ferroelectrics.⁵ Up and down hysteresis offsets were experimentally observed when temperature gradients were imposed across a bulk ferroelectric material. Conversely, there was no hysteresis offset in the absence of a temperature gradient, thereby conclusively establishing the origin of the observed behavior as intrinsic to the polarization gradient.

In this letter, we develop a theoretical model based on Landau–Ginzburg theory to analyze temperature-graded fer-

roelectrics. To link with prior experimental results, we confine our analysis to perovskite ferroelectric oxides exhibiting a cubic [Pm $\bar{3}$ m(#221)]–tetragonal [P4mm(#99)] phase transformation. For analysis, we consider a monodomain ferroelectric of thickness L sandwiched between two metallic electrodes, as illustrated in Fig. 1. The two electrodes are in contact with thermal sinks at temperatures T_1 and T_2 , imposing a temperature gradient across the ferroelectric bar. It is assumed that a steady state for heat transfer is established. The easy axis of polarization is along the z -axis such that $P_1 = P_2 = 0$, $P_3 = P = f(z)$, and the ferroelectric is considered to be chemically and thermally homogeneous along the x - and y -directions, reducing the problem to only one dimension. Accordingly, the Landau–Ginzburg–Devonshire free energy per unit area can be expressed by

$$F = \int_0^L \left[\frac{1}{2} \alpha P^2 + \frac{1}{4} \beta P^4 + \frac{1}{6} \gamma P^6 + \frac{1}{2} A \left(\frac{dP}{dz} \right)^2 - \frac{1}{2} E^D P - EP + F_{el}^i \right] dz, \quad (1)$$

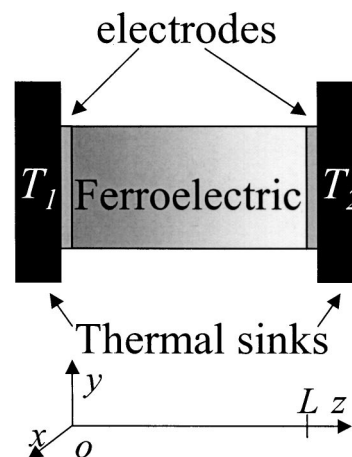


FIG. 1. Schematic diagram showing the setup of the temperature-graded ferroelectric and the coordinate used in the calculation.

^{a)}Author to whom correspondence should be addressed; electronic mail: p.alpay@ims.uconn.edu

where α , β , γ , and A are the free energy expansion coefficients. It is assumed that β and γ do not depend on the temperature. The temperature dependence of α is given by the Curie–Weiss law, $\alpha = (T - T_0)/\epsilon_0 C$, where T_0 and C are the Curie–Weiss temperature and constant, respectively, and ϵ_0 is the permittivity of free space. The gradient term represents additional energy from the nonuniform distribution of the polarization, serving to damp out spatial variations in polarization.^{6,7} The coefficient A can be approximated as $\delta^2|\alpha|$, where δ is the characteristic length along which the polarization varies. E is the external electric field along the z -direction and E^D is the depolarization field.⁸ We assume that the contribution of the depolarization field is negligible due to the small but finite conductivity of the material as well as local compensation by such defects as oxygen vacancies in perovskite ferroelectrics. The last term of Eq. (1), F_{el}^i , is the internal elastic energy resulting from variation of the lattice parameter within a temperature-graded, unconstrained ferroelectric bar. The total internal strain (in the contracted notation) in the xy -plane $x_1 = x_2 = x_{tot}$ is given by⁹

$$x_{tot}(z) = x_0(z) + (z - L/2)\kappa. \quad (2)$$

The first term in Eq. (2) represents the variation in the misfit in the xy -plane between a particular “layer” and the average self-strain, and is given by $x_0(z) = Q_{12}[P^2(z) - \langle P \rangle^2]$, where Q_{12} is the electrostrictive coefficient and $\langle P \rangle$ is the average polarization. The second term is the strain resulting from the bending moment due to the misfit between layers. κ is the radius of curvature of the bent ferroelectric bar, given by $\kappa = 24/L^3 \int_0^L (z - L/2)x_0(z) dz$. Thus, the internal elastic energy is

$$F_{el}^i(z) = \frac{1}{2}(\sigma_1 x_1 + \sigma_2 x_2) \\ = \bar{C}\{Q_{12}[P^2(z) - \langle P \rangle^2] + (z - L/2)\kappa\}^2, \quad (3)$$

using the mechanical boundary conditions $\sigma_1 = \sigma_2$, and $\sigma_3 = \sigma_4 = \sigma_5 = \sigma_6 = 0$, where σ_i are the components of the internal stress tensor, and $\bar{C} = (C_{11} + C_{12} - 2C_{12}^2/C_{11})$, where C_{ij} are the elastic constants at constant polarization.

The minimization of the free energy with respect to the polarization yields the Euler–Lagrange equation

$$A \frac{d^2 P}{dz^2} = \bar{\alpha} P + \bar{\beta} P^3 + \gamma P^5, \quad (4)$$

where $\bar{\alpha} = \alpha + 4\bar{C}Q_{12}[(z - L/2)\kappa - Q_{12}\langle P \rangle^2]$ and $\bar{\beta} = \beta + 4\bar{C}Q_{12}^2$. Assuming that steady-state heat transfer is established, the normalized coefficient $\bar{\alpha}$ in Eq. (4) becomes

$$\bar{\alpha} = \frac{L(T_1 - T_0) + z(T_2 - T_1)}{L\epsilon_0 C} + 4\bar{C}Q_{12}[(z - L/2)\kappa \\ - Q_{12}\langle P \rangle^2]. \quad (5)$$

The most extensive and systematic experimental study of the charge offset for temperature graded ferroelectrics was carried out by Fellberg *et al.*⁵ In their experiment, a 0.1-cm-thick $\text{Ba}_{0.75}\text{Sr}_{0.25}\text{TiO}_3$ (BST 75/25) ceramic was sandwiched between cold and hot temperature sinks. The cold sink temperature T_1 was fixed and hot sink temperature T_2 was varied. Experimentally, the susceptibility and the remnant polarization as a function of the temperature were mapped out for a homogeneous temperature distribution, $T_1 = T_2$. Sub-

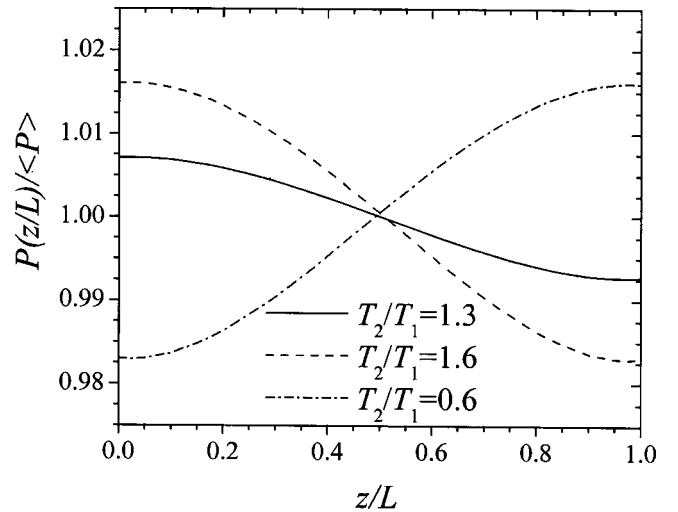


FIG. 2. Theoretical, normalized polarization profiles along the z -direction for temperature-graded $\text{Ba}_{0.75}\text{Sr}_{0.25}\text{TiO}_3$. T_1 and T_2 are the temperatures at each end of the ferroelectric bar. The dash-dotted line corresponds to the case in which a negative temperature gradient ($T_2/T_1 = 0.6$) is imposed on the ferroelectric bar.

sequently, the resulting charge offsets as a function of the temperature difference between the cold and hot sinks were measured. To perform the comparison between the calculation and experimental data, free-energy expansion coefficients α and β were retrieved from the experimentally determined susceptibility and the remnant polarization as a function of the temperature for homogeneous temperature distributions.¹⁰

Using the boundary conditions $dP/dz = 0$ at $z = 0$ and $z = L$ corresponding to charge compensation at the ferroelectric/electrode interfaces, we plot the normalized polarization with respect to average polarization $\langle P \rangle$ as a function of position for three different temperature gradients for BST 75/25 in Fig. 2 (T_1 is fixed at 35 °C if $T_2/T_1 > 1$; or T_2 is fixed at 35 °C if $T_2/T_1 < 1$). $P(z)$ is numerically obtained from Eqs. (4) and (5) using a finite difference method having an accuracy of (successive iterations) approximately 10^{-7} . As can be seen from Fig. 2, the normalized polarization varies monotonically along the z -direction. The polarization gradient diminishes close to the surfaces because of the boundary conditions. The magnitude and the direction of the polarization gradient depend on the temperature gradient imposed on the ferroelectric. If $T_2/T_1 > 1$, that is, if there is a positive temperature gradient along the z -direction, a continuously declining polarization profile is obtained. The polarization profile becomes steeper if temperature gradient is increased from $T_2/T_1 = 1.3$ (solid line) to $T_2/T_1 = 1.6$ (dashed line). The dash-dotted line in Fig. 2 corresponds to the case in which a negative temperature gradient ($T_2/T_1 = 0.6$) is imposed on the ferroelectric bar. In this case, the polarization profile is inverted in comparison to the positive temperature gradient.

The polarization profile then can be used to calculate the charge offset per unit area ΔQ from the one-dimensional Poisson equation: $\Delta Q = 1/L \int_0^L z(dP/dz) dz$,¹¹ which results in an internal (or built-in) field $E_i(z) = -[z/\epsilon_0 \epsilon_r(z)] dP/dz$. To evaluate the effect of the temperature gradient on the charge offset, we fix the temperature T_1

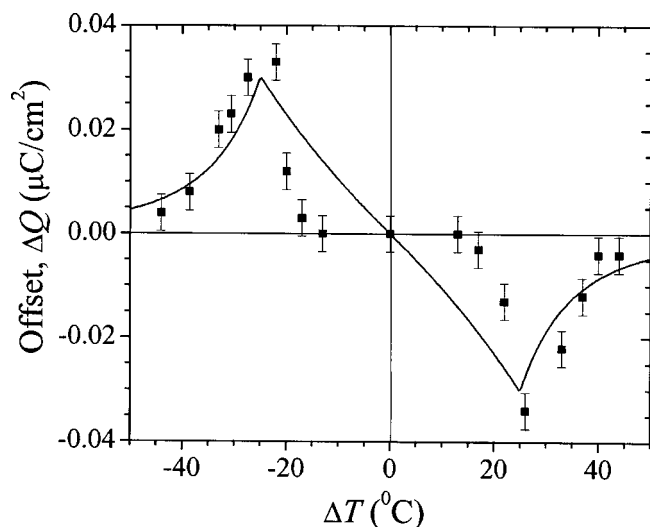


FIG. 3. Calculated charge offset as a function of the temperature difference ΔT between hot and cold sinks for temperature-graded $\text{Ba}_{0.75}\text{Sr}_{0.25}\text{TiO}_3$ (solid lines). Solid squares correspond to the experimental data taken from Ref. 5.

as a constant ($T_1 = 35^\circ\text{C}$) and vary the temperature T_2 ($T_2 \geq T_1$). In Fig. 3, we plot the charge offsets ΔQ as a function of the temperature difference $\Delta T = T_2 - T_1$ for temperature-graded BST 75/25 (solid lines). Figure 3 shows that the charge offset initially increases in a continuous fashion with increasing temperature difference ΔT as a result of the increasing polarization gradient. A maximum charge offset is obtained when hot sink temperature T_2 reaches a temperature at which the polarization varies most rapidly, although the material has not converted to a paraelectric. Further increase in the temperature leads to the formation of a paraelectric region within the ferroelectric bar with no spontaneous polarization. This paraelectric region expands with increasing T_2 , resulting in a decrease in the charge offset. An important feature predicted by our model is that the sign of the charge offset is reversed if that of the temperature grading is reversed (i.e., T_2 is fixed at 35°C , T_1 is a variable, and $T_1 \geq T_2$), as shown in the negative temperature difference region in Fig. 3.

The theoretical prediction of the charge offset for temperature-graded ferroelectrics is compared to the experimental results, as shown by the squares in Fig. 3. The agreement between the experimental data and theoretical calculation is quite remarkable, considering that there are no adjustable parameters in the theoretical analysis. It should be noted that, for small temperature gradients, the experimentally determined charge offsets are indistinguishable from the background variation. The small difference between the the-

oretical and experimental results may be explained by considering the clamping effect of the electrodes by the heat sinks. In the experimental measurement, the whole sample was under compression so as to maintain good thermal contact between the heat sinks. Consequently, as temperature gradients were established across the sample through heating, the sample expanded, resulting in an increase in the thermal stress, which in turn diminished the overall polarization.¹² The corresponding charge offset is, therefore, suppressed for very small temperature gradient. As it is quite difficult to accurately model the combined electromechanical setup without introducing a number of adjustable free parameters, we have not tried to directly account for this effect.

In conclusion, we have developed a Landau–Ginzburg thermodynamic model to analyze temperature-graded ferroelectrics. Polarization gradients with attendant charge offsets are predicted. Remarkable quantitative agreement between the theoretical calculations and the experimental data reported in the literature was found, validating the theoretical formalism.

We gratefully acknowledge helpful conversations with N. W. Schubring and A. L. Micheli of Delphi Research Laboratories and A. L. Roytburd of the University of Maryland. Two of the authors (Z.-G.B. and S.P.A.) also wish to acknowledge support from the National Science Foundation under Grant No. DMR-0132918 and the University of Connecticut Research Foundation.

- ¹J. V. Mantese and N. W. Schubring, *Integr. Ferroelectr.* **37**, 245 (2001).
- ²J. V. Mantese, N. W. Schubring, A. L. Micheli, M. S. Mohammed, R. Naik, and G. W. Auner, *Appl. Phys. Lett.* **71**, 2047 (1997).
- ³M. Brazier, M. McElfresh, and S. Mansour, *Appl. Phys. Lett.* **72**, 1121 (1998).
- ⁴D. Bao, N. Mizutani, L. Zhang, and X. Yao, *J. Appl. Phys.* **89**, 801 (2001).
- ⁵W. Fellberg, J. V. Mantese, N. W. Schubring, and A. L. Micheli, *Appl. Phys. Lett.* **78**, 524 (2001).
- ⁶L. P. Kadanoff, W. Gotze, D. Hamblen, R. Hecht, E. A. S. Lewis, V. V. Paiciauskas, M. Rayl, J. Swift, D. Aspnes, and J. Kane, *Rev. Mod. Phys.* **39**, 395 (1967).
- ⁷L. D. Landau and E. M. Lifshitz, *Statistical Physics* (Pergamon, Oxford, 1980).
- ⁸R. Kretschmer and K. Binder, *Phys. Rev. B* **20**, 1065 (1979).
- ⁹A. L. Roytburd and J. Slutsker, *Acta Mater.* **50**, 1809 (2002).
- ¹⁰The list of parameters (in SI units, T in $^\circ\text{C}$) for $\text{Ba}_{0.75}\text{Sr}_{0.25}\text{TiO}_3$, $\alpha = 1.12(T-60) \times 10^6$, $\beta = 1.3 \times 10^{11}$ [α and β for $\text{Ba}_{0.75}\text{Sr}_{0.25}\text{TiO}_3$ were retrieved from Figs. 1 and 2 in Ref. 5], $C_{11} = 2.19 \times 10^{11}$, $C_{12} = 0.88 \times 10^{11}$, and $Q_{12} = -0.034$ (C_{11} , C_{12} , and Q_{12} were compiled from T. Mitsui, I. Tatsuzaki, and E. Nakamura, in *An Introduction to the Physics of Ferroelectrics* (Gordon and Breach, New York, 1974); Z.-G. Ban and S. P. Alpay, *J. Appl. Phys.* **91**, 9288 (2002).
- ¹¹Z. Chen, K. Arita, M. Lim, and C. A. P. Araujo, *Integr. Ferroelectr.* **24**, 181 (1999).
- ¹²F. Jona and G. Shirane, *Ferroelectric Crystals* (Dover, New York, 1962), p. 21.